Electronic Supplementary Material (ESI) for Journal of Materials Chemistry C.

Kinetic Condition Driven Phase and Vacancy Control Enhancing Thermoelectric Performance of Nano-sized Low-cost and Eco-friendly $Cu_{2-x}S$

Wei-Di Liu,[a] Xiao-Lei Shi,[a] Han Gao,[a] Raza Moshwan,[a] Sheng-Duo Xu,[a] Yuan Wang,[b,a] Lei Yang,[c] Zhi-Gang Chen[b,a] Jin Zou[a,d,]**

[a]Materials Engineering, The University of Queensland, Brisbane, Queensland 4072, Australia.

[b]Centre for Future Materials, University of Southern Queensland, Springfield central, Queensland 4300, Australia.

[c]School of Materials Science and Engineering, Sichuan University, Chengdu 610065, China

[d]Centre for Microscopy and Microanalysis, The University of Queensland, Brisbane, Queensland 4072, Australia.

1. Experimental details

Material preparation: The $Cu_{2-x}S$ powders were synthesized by a facile solvothermal method. CuO (98%), S (99%), NaOH (97%) and ethylene glycol (99%) were employed as the precursors (purchased from Sigma Aldrich). Detailed synthesis mechanism can be express as:

$$12\ CuO + 3\ C_2H_6O_2 = 12\ Cu^+ + 3\ C_2H_2O_2 + 12\ OH^- \quad (1)$$

$$8\ S + 16\ OH^- = 6\ S^{2-} + 2\ SO_4^{2-} + 8\ H_2O \quad (2)$$

$$12\ Cu^+ + 6\ S^{2-} = 6\ Cu_2S \quad (3)$$

In total, the reaction mechanism can be summarized as:

$$12\ CuO + 3\ C_2H_6O_2 + 8\ S + 4\ OH^- = 2\ SO_4^{2-} + 8\ H_2O + 3\ C_2H_2O_2 + 6\ Cu_2S \quad (4)$$

NaOH solution (10 mol L^{-1}) was employed to adjust the reaction kinetic condition by changing the acid-base environment. More NaOH can boost the formation of $Cu_{2-x}S$ phases. In each synthesis process, 36 ml ethylene glycol and varying amount of NaOH solution (2, 4 and 6 ml) were sufficiently mixed in a 125 ml Teflon container under the stirring speed of 500 r/min. Then, 0.020 mol CuO and 0.016 mol S were added into the solution under continuous stirring. The container was subsequently sealed in a stainless-steel autoclave, heated up to 230 ℃, kept for 24 h and slowly cooled to room-temperature. The as-synthesized powders were collected by centrifuging, washed by ethanol and de-ionized water several times and subsequently dried at 60 ℃ for ~12 h. For performance measurement, as-synthesized powders were sintered into pellets by spark plasma sintering (Fuji-211Lx) under 550 ℃ for 5 min.

Thermoelectric performance measurement: To identify the electrical performance, the Seebeck coefficient (S) and electrical conductivity (σ) were measured simultaneously by both ZEM3 (ULVAC) and SBA 458 (NETZSCH). To understand the thermal performance, the total thermal conductivity (κ) was calculated based on $\kappa = \rho \cdot Cp \cdot D$, where the ρ, C_p and D are the density, specific heat and thermal diffusivity, respectively. The ρ of all bulks were measured by Archimedes method and higher than 98%. The C_p was measured by DSC 404 F3 (NETZSCH). The D was measured by both LFA 457 (NETZSCH) and LFA 467 (HyperFlash, NETZSCH). To

understand the carrier transport properties, the n_H was measured by the van der Pauw technique under a reversible magnetic field of ±1.5 T. All thermoelectric performance were measured perpendicular to the pressing direction.

Table S1. Measured densities of as-prepared $Cu_{2-x}S$ pellets

NaOH amount	Density	Relative density
2 ml	5.50 g/cm^3	98 %
4 ml	5.54 g/cm^3	99 %
6 ml	5.55 g/cm^3	99 %

Structural Characterization: The room-temperature structural information of as-synthesized bulks were collected by a Bruker D8 advanced powder X-ray diffraction (XRD). Rigaku Smart Lab thin-film and micro-diffraction XRD was employed for In situ heating XRD. Both equipment are equipped with graphite monochromatized Cu Kα radiation source (λ = 0.15408 nm). The Rietveld refinement (MAUD) was carried out for phase content analysis. The crystal structure was further confirmed by Transmission electron microscopy (Philips Tecnai F20 FEG-S/TEM) on a specimen cut from the sintered pellet ($Cu_{2-x}S$ synthesized with 4 ml NaOH) by Ultramicrotone. The composition was statistically analyzed via both energy dispersive X-ray spectroscopy (EDS, Hitachi SU3500) and electron probe micro-analyzer (EPMA, JXA-8200).

2. Single parabolic band model calculation

Thermoelectric parameters of as-prepared $Cu_{2-x}S$ samples could be calculated based on single parabolic band (SPB) model:[1-3]

$$S(\eta) = \frac{k_B}{e} \cdot \left[\frac{\left(r + \frac{5}{2}\right) \cdot F_{r+\frac{3}{2}}(\eta)}{\left(r + \frac{3}{2}\right) \cdot F_{r+\frac{1}{2}}(\eta)} - \eta \right] \tag{5}$$

$$n_H = \frac{1}{e \cdot R_H} = \frac{(2m^* \cdot k_B T)^{\frac{3}{2}}}{3\pi^2 \hbar^3} \cdot \frac{\left(r + \frac{3}{2}\right)^2 \cdot F^{\,2}_{r+\frac{1}{2}}(\eta)}{(2r + \frac{3}{2}) \cdot F_{2r+\frac{1}{2}}(\eta)} \tag{6}$$

$$\mu_H = \left[\frac{e\pi\hbar^4 \quad C_l}{\sqrt{2}(k_B T)^{\frac{3}{2}} E_{def}{}^2 (m^*)^{\frac{5}{2}}} \right] \frac{(2r + \frac{3}{2}) \cdot F_{2r+\frac{1}{2}}(\eta)}{\left(r + \frac{3}{2}\right)^2 \cdot F_{r+\frac{1}{2}}(\eta)} \tag{7}$$

$$L = (\frac{k_B}{e})^2 \cdot \left\{ \frac{\left(r + \frac{7}{2}\right) \cdot F_{r+\frac{5}{2}}(\eta)}{\left(r + \frac{3}{2}\right) \cdot F_{r+\frac{1}{2}}(\eta)} - \left[\frac{\left(r + \frac{5}{2}\right) \cdot F_{r+\frac{3}{2}}(\eta)}{\left(r + \frac{3}{2}\right) \cdot F_{r+\frac{1}{2}}(\eta)} \right]^2 \right\} \tag{8}$$

where η, k_B, e, r, R_H, m^*, $\hbar$, C_l and E_{def} are the reduced Fermi level, the Boltzmann constant, the elementary charge, the carrier scattering factor (r = -1/2 for acoustic phonon scattering),[2] the Hall coefficient, the effective mass, the reduced Plank constant, the elastic constant for longitudinal vibrations and the deformation potential coefficient, respectively. Here $C_l = v_l^2 \cdot \rho$, where v_l =3711 m·s^{-1} is the longitudinal sound velocity.[4] $F_i(\eta)$ is the Fermi integral and can be expressed as

$$F_i(\eta) = \int_0^\infty \frac{x^i}{1 + e^{(x-\eta)}} dx \tag{9}$$

3. Rietveld refinement of room-temperature XRD patterns of as-prepared $Cu_{2-x}S$ bulks

To clearly reveal the existence and change of individual $Cu_{2-x}S$ phases, enlarged XRD peaks of $Cu_{2-x}S$ pellets sintered from powders synthesized with different amount of NaOH are shown in **Figure S1**a. As can be seen, intensity of characteristic peaks of the Cu_2S reduced with the

reducing amount of NaOH indicating reducing amount of the Cu_2S phase. On the contrary, peak intensity of the $Cu_{1.94}S$ phase has dramatically increased with the reducing amount of NaOH indicating increasing amount of the $Cu_{1.94}S$ phase. Peak intensity of the $Cu_{1.96}S$ phase has obviously increased with the NaOH amount reducing from 6 ml to 4 ml and remains similar when further reducing to 2 ml, this reveals that the amount of $Cu_{1.96}S$ phase has sharply increased while the NaOH amount has reduced from 6 ml to 4 ml and remains one of the major component when the NaOH amount further reduced to 2 ml. This result is closely consistent with the Rietveld refinement result (**Figure 2**b). Additionally, note that the compositional difference between these three phases is quite small. As for this reason, under the same crystal growth condition during the synthesis process, kinetic-condition driven composition change would lead to different formation energy and subsequently changed crystal structure. Hence, composition of the same $Cu_{2-x}S$ phase should be similar.

To analyze the phase contents, Rietveld refinement was carried out. The experimental and calculated patterns are shown in **Figure. S1**b. As can be seen, the calculated and experimental patterns are consistent with each other. The R_{wp} and χ^2 values of all samples are smaller than 4.0 and 2, respectively, indicating reliable refinement.

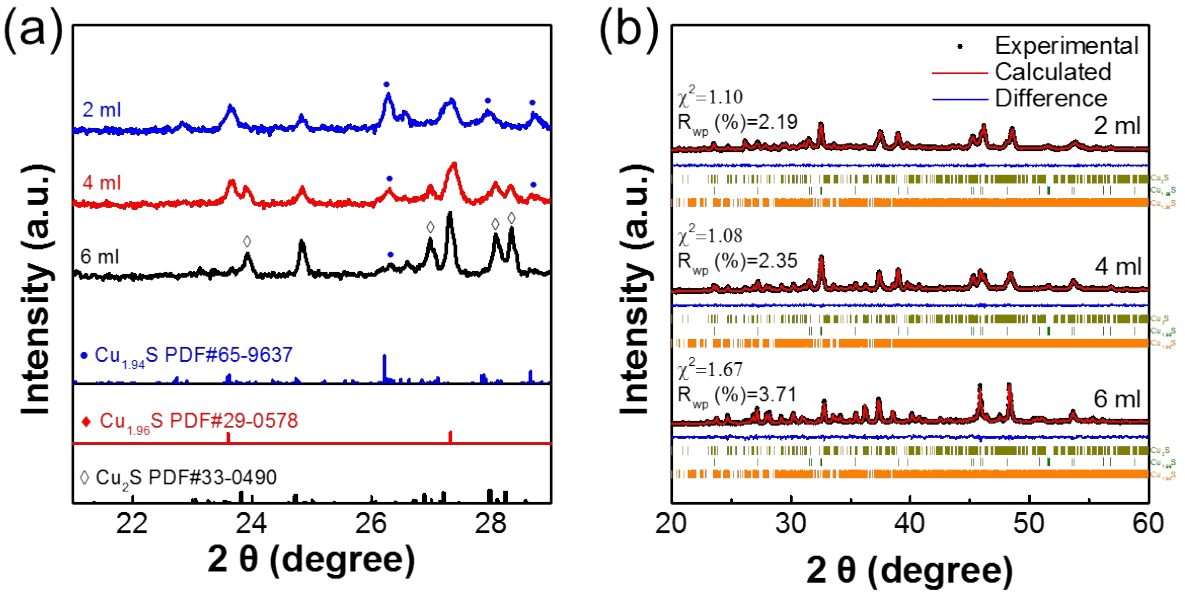

Figure S1. (a) Enlarged XRD peaks of the $Cu_{2-x}S$ pellets sintered from powders synthesized with 2, 4 and 6 ml NaOH, respectively; (b) Rietveld refinement calculated XRD patterns in comparison with the experimental ones.

4. Lorenz factor of as-prepared $Cu_{2-x}S$ pellets

Figure S2 shows the SPB-calculated Lorenz factor (L) of as-prepared $Cu_{2-x}S$ pellets. With increasing amount of NaOH, the L has reduced due to enhanced n_H (**Figure 3b**).

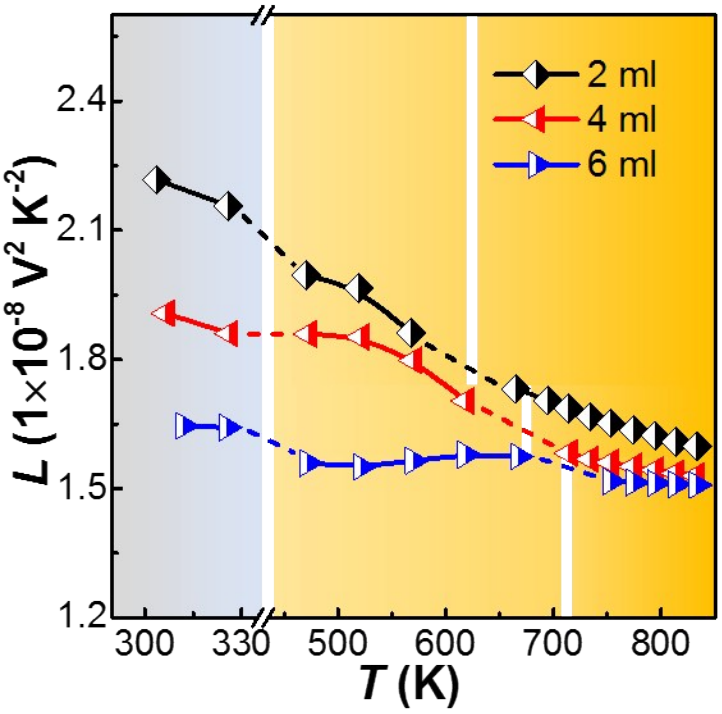

Figure S2. The SPB model-calculated Lorenz factor (L).

5. Influence of reduced phase transition temperature on thermoelectric performance of as-prepared $Cu_{2-x}S$

To understand the influence of reduced phase transition temperature on thermoelectric performance, σ, S, $S^2\sigma$, κ, lattice thermal conductivity (κ_l) and zT of the $Cu_{2-x}S$ pellet sintered from powders synthesized with 2 ml NaOH were aligned to the given phase transition temperature of 715 K, and shown in **Figure S3** in comparison with the original one. As can be seen from **Figure S3**a, due to early appearance of high-temperature and high-performance cubic $Cu_{2-x}S$ at 630 K rather than 715 K, σ is enhanced when the temperature is below 700 K. Simultaneously, σ above 700 K has dropped. It should be noted that σ below and above 700 K show different trends with reduced phase transition temperature due to different temperature-dependency behaviours before and after the phase transition at ~700 K of $Cu_{2-x}S$. Meanwhile, as

n_H remains nearly temperature-independent (**Figure 3**b), this should be mainly attributed to changed carrier mobility (μ_H, **Figure 3**c). The early appearance of cubic $Cu_{2-x}S$ with higher S at 630 K has also led to the enhanced S (**Figure S3**b). Due to simultaneously enhanced σ and S below 700 K, **Figure S3**c shows the enhanced $S^2\sigma$. Above 700 K, dominated by enhanced S, $S^2\sigma$ of the $Cu_{2-x}S$ pellets have also been slightly enhanced. Similar to the σ tendency, the reduced phase transition temperature has also led to slightly enhanced κ below 700 K, but reduced κ above 700 K, as shown in **Figure S3**d. The change in κ is dominated by the changed electrical thermal conductivity (κ_e) as κ_l has no obvious change (**Figure S3**e). Overall, with reducing phase transition temperature, zT of the $Cu_{2-x}S$ pellet is enhanced (**Figure S3**f).

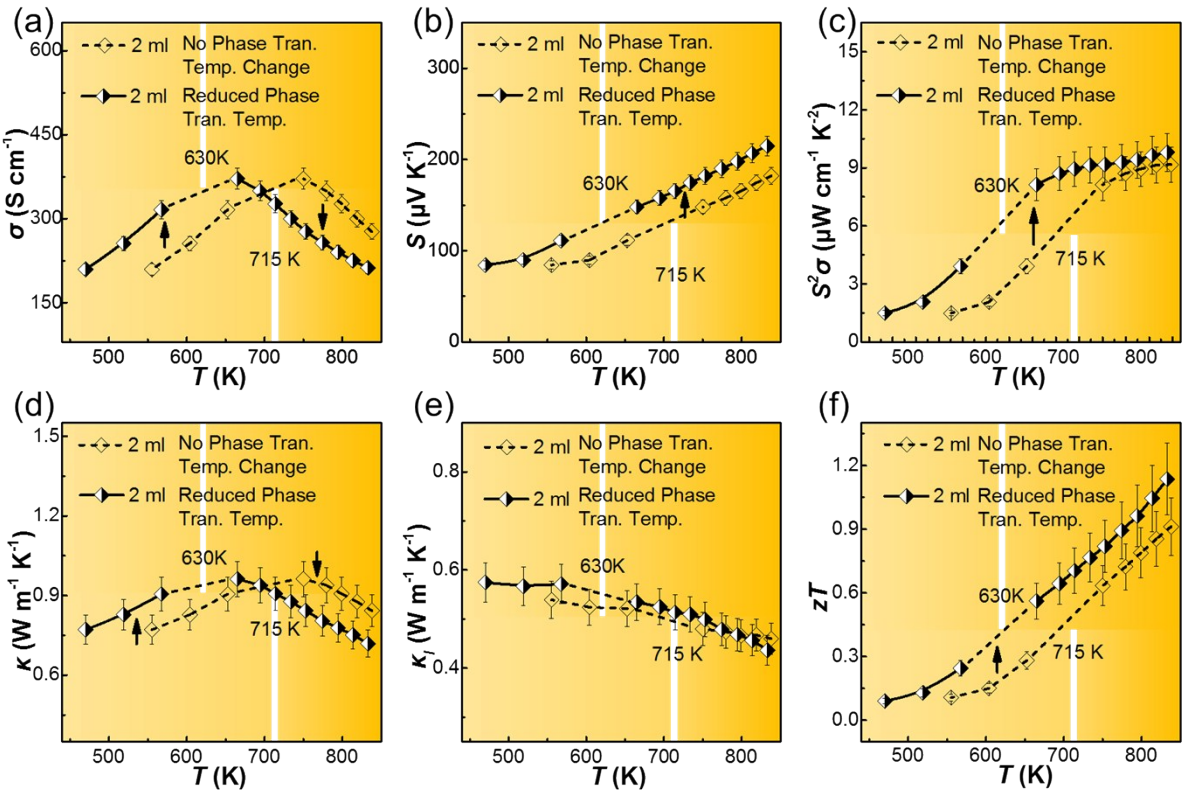

Figure S3. The temperature-dependent thermoelectric performance (>473 K) with the phase transition temperature being defined at ~715 K in comparison with the true phase transition temperatures (taking the $Cu_{2-x}S$ pellet sintered from powders synthesized with 2 ml NaOH whose

phase transition temperature has reduced to ~630 K in comparison with the 6 ml one), including (a) electrical conductivity (σ), (b) Seebeck coefficient (S), (c) power factor ($S^2\sigma$), (d) total thermal conductivity (κ), (e) lattice thermal conductivity (κ_l) and (f) dimensionless figure of merit (zT).

6. Composition analysis of as-sintered $Cu_{2-x}S$ pellets

Detailed electron probe micro-analyzer (EPMA) composition analysis of $Cu_{2-x}S$ pellets sintered from powders synthesized with 2, 4 and 6 ml of NaOH, respectively, are shown in the **Table S2**, **S3** and **S4**. As the composition of three $Cu_{2-x}S$ phases are closely within the error range, they can be hardly identified via composition analysis.

Table S2. EPMA measured composition of as-prepared $Cu_{2-x}S$ pellets sintered from powders synthesized with 2 ml NaOH

Point	Cu (at. %)	S (at. %)	Total (at. %)	Cu/S
2ml-1	66.0345	33.9655	100	1.944164
2ml-2	66.1258	33.8742	100	1.952099
2ml-3	66.0468	33.9532	100	1.94523
2ml-4	66.2315	33.7685	100	1.96134
2ml-5	65.9856	34.0144	100	1.939931
2ml-6	66.0345	33.9655	100	1.944164
2ml-7	65.8941	34.1059	100	1.932044
2ml-8	66.3158	33.6842	100	1.968751
2ml-9	66.1795	33.8205	100	1.956787
2ml-10	66.3843	33.6157	100	1.9748
2ml-11	66.3138	33.6862	100	1.968575
2ml-12	65.9057	34.0943	100	1.933042
2ml-13	66.2844	33.7156	100	1.965986
2ml-14	66.3157	33.6843	100	1.968742
2ml-15	66.2098	33.7902	100	1.959438
2ml-16	66.2871	33.7129	100	1.966224
2ml-17	66.1053	33.8947	100	1.950314
2ml-18	66.2337	33.7663	100	1.961533
2ml-19	66.0567	33.9433	100	1.94609

2ml-20	65.9317	34.0683	100	1.93528
average	66.14382	33.85619	100	1.953727

Table S3. EPMA measured composition of as-prepared $Cu_{2-x}S$ pellets sintered from powders synthesized with 4 ml NaOH

Point	Cu (at. %)	S (at. %)	Total (at. %)	Cu/S
4ml-1	66.3528	33.6472	100	1.972016
4ml-2	66.0513	33.9487	100	1.945621
4ml-3	66.0358	33.9642	100	1.944277
4ml-4	66.6432	33.3568	100	1.997889
4ml-5	66.2251	33.7749	100	1.960779
4ml-6	66.4384	33.5616	100	1.979596
4ml-7	66.2272	33.7728	100	1.960963
4ml-8	65.9841	34.0159	100	1.939802
4ml-9	66.3586	33.6414	100	1.972528
4ml-10	66.5532	33.4468	100	1.989823
4ml-11	66.0631	33.9369	100	1.946645
4ml-12	66.5271	33.4729	100	1.987491
4ml-13	66.4198	33.5802	100	1.977945
4ml-14	66.2366	33.7634	100	1.961787
4ml-15	66.0574	33.9426	100	1.94615
4ml-16	65.9135	34.0865	100	1.933713
4ml-17	67.2818	32.7182	100	2.056403
4ml-18	66.4795	33.5205	100	1.983249
4ml-19	66.5354	33.4646	100	1.988232
4ml-20	66.3682	33.6318	100	1.973376
average	66.33761	33.6624	100	1.970914

Point	Cu %	S %	Total %	Cu/S
4ml-1	66.3528	33.6472	100	1.972016
4ml-2	66.0513	33.9487	100	1.945621
4ml-3	66.0358	33.9642	100	1.944277
4ml-4	66.6432	33.3568	100	1.997889
4ml-5	66.2251	33.7749	100	1.960779
4ml-6	66.4384	33.5616	100	1.979596
4ml-7	66.2272	33.7728	100	1.960963
4ml-8	65.9841	34.0159	100	1.939802
4ml-9	66.3586	33.6414	100	1.972528
4ml-10	66.5532	33.4468	100	1.989823
4ml-11	66.0631	33.9369	100	1.946645
4ml-12	66.5271	33.4729	100	1.987491
4ml-13	66.4198	33.5802	100	1.977945

4ml-14	66.2366	33.7634	100	1.961787
4ml-15	66.0574	33.9426	100	1.94615
4ml-16	65.9135	34.0865	100	1.933713
4ml-17	67.2818	32.7182	100	2.056403
4ml-18	66.4795	33.5205	100	1.983249
4ml-19	66.5354	33.4646	100	1.988232
4ml-20	66.3682	33.6318	100	1.973376
average	66.33761	33.6624	100	1.970914

Table S4. EPMA measured composition of as-prepared $Cu_{2-x}S$ pellets sintered from powders synthesized with 6 ml NaOH

Point	Cu %	S %	Total %	Cu/S
6ml-1	66.3596	33.6404	100	1.972616
6ml-2	66.5878	33.4122	100	1.992919
6ml-3	66.4591	33.5409	100	1.981435
6ml-4	66.5755	33.4245	100	1.991817
6ml-5	66.5283	33.4717	100	1.987598
6ml-6	66.4713	33.5287	100	1.982519
6ml-7	66.6905	33.3095	100	2.002147
6ml-8	66.4188	33.5812	100	1.977857
6ml-9	66.5271	33.4729	100	1.987491
6ml-10	66.6281	33.3719	100	1.996533
6ml-11	66.5198	33.4802	100	1.98684
6ml-12	66.5384	33.4616	100	1.9885
6ml-13	66.6971	33.3029	100	2.002742
6ml-14	66.4315	33.5685	100	1.978983
6ml-15	66.4952	33.5048	100	1.984647
6ml-16	66.5795	33.4205	100	1.992175
6ml-17	66.6312	33.3688	100	1.996811
6ml-18	66.4058	33.5942	100	1.976704
6ml-19	66.4792	33.5208	100	1.983222
6ml-20	66.459	33.541	100	1.981426
average	66.52414	33.47586	100	1.987249

Reference

1. Y. Xu, W. Li, C. Wang, J. Li, Z. Chen, S. Lin, Y. Chen and Y. Pei, *J. Mater. Chem. A*, 2017, **5**, 19143-19150.
2. J. Shen, Z. Chen, S. lin, L. Zheng, W. Li and Y. Pei, *J. Mater. Chem. C*, 2016, **4**, 209-214.

3. X. She, X. Su, H. Du, T. Liang, G. Zheng, Y. Yan, R. Akram, C. Uher and X. Tang, *J. Mater. Chem. C*, 2015, **3**, 12116-12122.
4. Y. He, T. Day, T. Zhang, H. Liu, X. Shi, L. Chen and G. J. Snyder, *Adv. Mater.*, 2014, **26**, 3974-3978.